Parallel excitation of hole and electron intersubband resonances in space-charge layers on silicon

A. D. Wieck, E. Batke, D. Heitmann, and J. P. Kotthaus
Institut für Angewandte Physik, Universität Hamburg, Jungiusstrasse 11, D-2000 Hamburg 36, West Germany
(Received 5 January 1984; revised manuscript received 3 April 1984)

Intersubband resonances are investigated in hole space-charge layers on Si(111), Si(100), and Si(110), and in electron space-charge layers on Si(110) and Si(111). The resonances are excited by far-infrared radiation with the electric field vector polarized parallel to the interface. We report on frequency domain studies covering a wide range of frequencies (50—1000 cm^{-1}) and charge densities [$(1-14)\times10^{12}$ cm^{-2}]. We have investigated resonance positions, line shapes, excitation strengths, polarization dependence, and the influence of depletion fields. Results are compared with available theories on hole and electron subband systems.

I. INTRODUCTION

Holes or electrons, which are confined by a surface electric field in a narrow potential well at the interface of a metal-oxide-silicon (MOS) device, are free to move parallel to the interface, but the motion perpendicular to the surface (z direction) is quantized.[1] The energy spectrum of this quasi-two-dimensional (2D) system thus consists of a set of subbands (index i) with energy dispersion $E_i(k_x,k_y)$. A detailed knowledge of subband energies and dispersions is of fundamental interest for 2D systems. A powerful tool for the investigation of the subband separations is the spectroscopic study of resonant intersubband transitions (e.g., Ref. 2). For electron inversion and accumulation layers a great body of theoretical (e.g., Refs. 1 and 3—5) and experimental work (e.g., Refs. 6 and 7) exists, most of which concentrates on the (100) surface of Si at low charge densities $N_s<3\times10^{12}cm^{-2}$.

Considerably less information has been published for subband energies in hole space-charge layers of Si. The valence bands of bulk Si are complex and hole subband energies can only be calculated by taking the mixing of the three highest valence bands into account. Self-consistent Hartree calculations have been carried out independently by Bangert *et al.*[8] and Ohkawa and Uemura.[9,10] In contrast to electron subbands, only little experimental data for hole space-charge layers exist; these data have been extracted from laser measurements[6,11] and are limited to low energies and charge densities. Currently, there is an increasing interest in more detailed studies of hole intersubband resonances using Raman[12—14] and Fourier-transform spectroscopy.[15]

The excitation of intersubband resonances characterizes the oscillatory motion of charge carriers perpendicular to the surface. In highly symmetrical systems, e.g., electrons on Si(100), excitation of intersubband resonance is only possible for radiation with an electric field component E_z normal to the surface. To induce a sufficiently large E_z component, special experimental configurations such as prism arrangements,[7] transmission lines,[6] or grating couplers[16] are necessary. These arrangements, however, reduce sensitivity and make an absolute determination of intersubband-resonance strengths difficult or impossible.

On semiconductors with ellipsoidal constant-energy contours and surfaces tilted with respect to the principal axis of these ellipsoids,[17,18] and on semiconductors with warped—or nonparabolic—band structure, the motion of charge carriers perpendicular and parallel to the surface is coupled. In this case an excitation of intersubband resonances with a parallel component of the electric field becomes possible and the excitation of intersubband resonances can be observed directly in the transmission of normally incident radiation. This allows very simple and sensitive experimental arrangements and facilitates a straightforward determination of the strength of intersubband excitations.

Here we present an extensive experimental investigation of intersubband resonances on Si in parallel excitation. We cover both a large frequency (50—1000 cm^{-1}) and charge-density regime ($N_s=1\times10^{12}$ to 14×10^{12} cm^{-2}). For intersubband resonances of holes on Si(100), Si(110), and Si(111) we report new transitions, polarization-dependent measurements, and substrate-bias experiments. Resonance positions are compared with available calculations.[8—10] We also present experimental data for intersubband transitions of electrons on Si(110) and Si(111). Our experiments are performed using Fourier-transform spectroscopy. These frequency-domain studies allow a detailed analysis of resonance positions, line shapes, and excitation strengths in absolute units.

II. SAMPLE CHARACTERIZATION AND EXPERIMENTAL TECHNIQUES

The experiments are performed on MOS capacitors with semitransparent gates typically 3—5 mm in diameter and with a gate impedance of 1000 Ω/□. The thickness of the thermally grown oxide ranges from 45 to 200 nm. The resistivity of most substrates ranges from 10 to 20 Ω cm, and some samples have a resistivity of 1000 Ω cm. Both p- and n-type substrates have been investigated. Experiments are carried out for accumulation of the charge

carriers, for quasiaccumulation, which is induced by illuminating the sample with band-gap radiation, for inversion, and with depletion fields, which are induced by a substrate-bias voltage. Temperatures in all experiments were about 20 K unless stated otherwise.

The excitation of intersubband transitions is observed in the relative change of transmission,

$$\Delta T/T=[T(V_G)-T(V_T)]/T(V_T)\ ,$$

for far-infrared radiation transmitted normally through the MOS sample with a semitransparent metal gate. $T(V_G)$ and $T(V_T)$ are the transmission through the sample at gate voltage V_G and at the conductivity-threshold voltage V_T, respectively. In the small-signal limit, $-\Delta T/T$ is proportional to the real part of the high-frequency conductivity of the space-charge layer (e.g., Refs. 1, 19, and 20). The backside of the sample is wedged to avoid interference effects. The experiments are performed using rapid-scan Fourier-transform spectroscopy. This method makes special spectroscopic techniques possible. Alternatingly, we measure interferograms I of the transmitted radiation at gate voltage V_G and threshold voltage V_T. The digitized interferograms $I(V_G)$ and $I(V_T)$ are co-added in different files and are Fourier-transformed separately at the end of the measurement. In this way the effective delay between measuring the spectrum $T(V_G)$ and the reference $T(V_T)$ is small (typically 1 to 10 s), and long-time drifts of the experimental setup are eliminated. Thus very weak relative changes of the transmission can be measured with a sufficient signal-to-noise ratio. A detailed description of the spectroscopy is given in Ref. 20. The quantity $\Delta T/T$ is measured in absolute units and can be compared directly with theoretical excitation strengths. Extensive measurements have been performed on different samples of each orientation and substrate doping in the frequency regime 50 to 380 cm^{-1}. During the later course of our investigations we also made measurements above 380 cm^{-1} using a Ge:Cu photoconductive element instead of a Ge bolometer. In all measurements made here the resolution was set to 4 cm^{-1}.

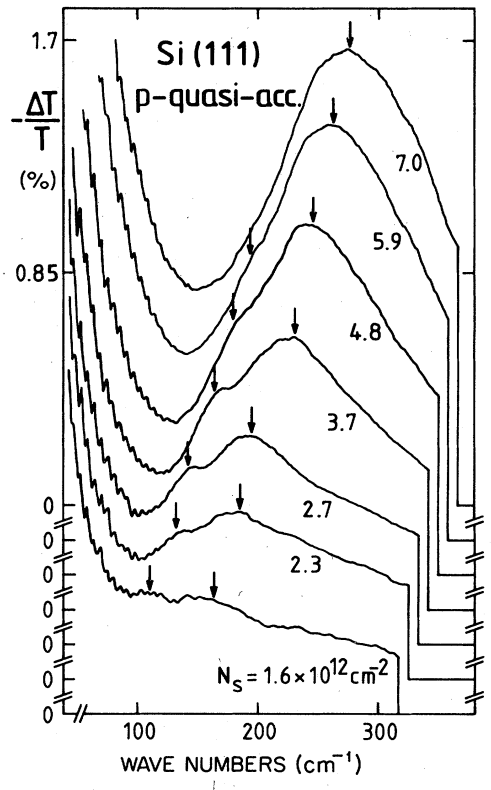

FIG. 1. Original experimental spectra of the relative change in transmission $-\Delta T/T$ caused by an accumulation layer of holes with different charge densities N_s on Si(111). Spectra are measured for normally transmitted far-infrared radiation, i.e., with the electric field vector parallel to the surface ("parallel excitation"). The intersubband-resonance transitions are marked by arrows.

III. INTERSUBBAND RESONANCE OF HOLES

A. Experimental results

1. Si(111)

The spectra for different surface orientations have many common features which will be discussed for the Si(111) surface. Special properties for Si(100) and Si(110) are described below. Original experimental spectra for accumulation of holes on Si(111) at different charge densities N_s are shown in Fig. 1. These spectra, which represent the real part of the high-frequency conductivity, consist of two contributions: intrasubband and intersubband transitions. The intrasubband contribution is Drude type and decreases approximately in proportion to $(\omega\tau)^{-2}$ with frequency, if $\omega\tau \gtrsim 1$, as is the case here. τ is the intraband scattering time. In the following we will refer to this intraband contribution as the "Drude background." The intersubband contribution in Fig. 1 is comparatively strong and consists of a broad resonance and a small, sharper resonance at low frequencies which is well pronounced, especially at low densities. Both resonances shift with increasing charge density to higher wave numbers. A third resonance is observed in the frequency regime 500 to 600 cm^{-1}, which is not shown in Fig. 1. Spectra measured with linearly polarized radiation are, within the experimental accuracy, identical for different directions of the electric field vector in the surface, as expected for an optically isotropic surface. It is characteristic for the hole intersubband resonances of all surface orientations that the half-width of the resonance ΔE is much broader than an energy half-width $2\hbar/\tau$ deduced from the Drude scattering time τ, which is measured for the same sample and charge density. The resonance line shape is significantly asymmetric, being broader on the high-frequency side. This can be clearly extracted from these frequency sweeps by substracting the 2D Drude background, at least at low densities. Within the accuracy of substracting this background, the weak, low-energy transitions in Fig. 1 seem to have a smaller width and a more symmetric profile. Asymmetry has also been deduced from N_s sweeps[6] and Raman spectroscopy.[12] The widths of the resonance and asymmetry have been inter-

preted as being caused by the nonparabolicity of the hole subbands. This interpretation seems to be supported by the fact that the line shape is not significantly affected by depletion fields, as discussed below.

2. *Inversion and substrate-bias experiments*

We have investigated hole intersubband resonances in both accumulation layers on *p*-type samples and band-gap-radiation—induced quasiaccumulation layers on *n*-type substrates, without measuring a significant difference in the resonance position and line shape. On *n*-type samples, which are illuminated with band-gap radiation, the photoexcited carriers prevent the formation of a depletion layer. Using a method described in more detail in Ref. 20, we are able to measure at inversion conditions and with substrate-bias voltages on MOS capacitors without source-drain contacts. In essence, synchronously with the mirror scans of the Fourier-transform spectrometer, the band-gap illuminated MOS capacitor is charged at a certain voltage V_C. Before the sampling of the interferogram starts, the illumination is switched off and an additional substrate-bias voltage is added to V_C. Without illumination, a depletion layer is formed and the electric field in the depletion layer can be varied by the substrate-bias voltage. The charge density N_{depl} of the depletion layer can be calculated from the substrate doping and substrate-bias voltage.[21]

In Fig. 2 we show experimental spectra for accumulation, inversion, and different depletion fields with corresponding depletion charges for Si(111). The positions of the main resonance and low-energy shoulder shift with increasing depletion field to higher frequencies, as is expected from the narrowing of the surface potential well. The low-energy shoulder decreases in intensity with increasing depletion field. The sample shown in Fig. 2 has a relatively low substrate doping ($|N_A - N_D| = 10^{13}$ cm^{-3}, resistivity 1000 Ω cm). On samples with higher substrate doping (20 Ω cm), higher depletion fields can be achieved and show, correspondingly, a more pronounced shift of the resonance. On both types of samples we find that for Si(111) the resonance profile and width are little affected by a depletion field, in contrast to experiments in electron space-charge layers. Thus for Si(111) we have no evidence that the half-width of the hole intersubband resonance is caused by several overlapping transitions due to accumu-

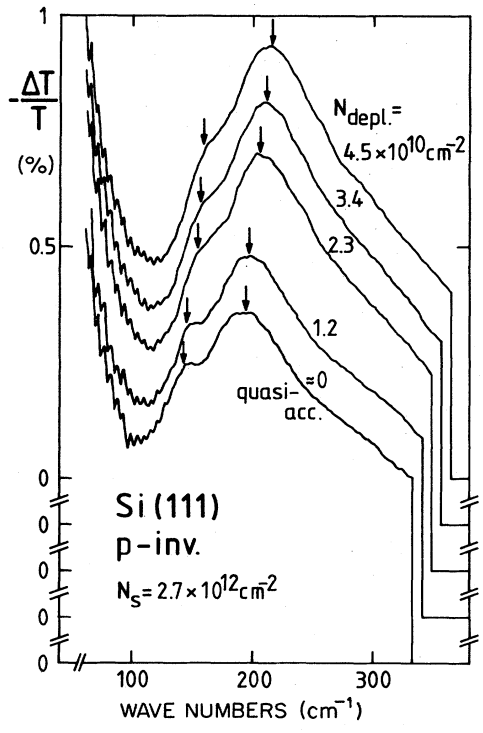

FIG. 2. Original experimental spectra $-\Delta T/T$ versus wave number on Si(111) for quasiaccumulation, inversion, and different depletion fields, which are induced by a substrate-bias voltage. The corresponding depletion charge N_{depl} is entered. Intersubband-resonance positions are marked by arrows.

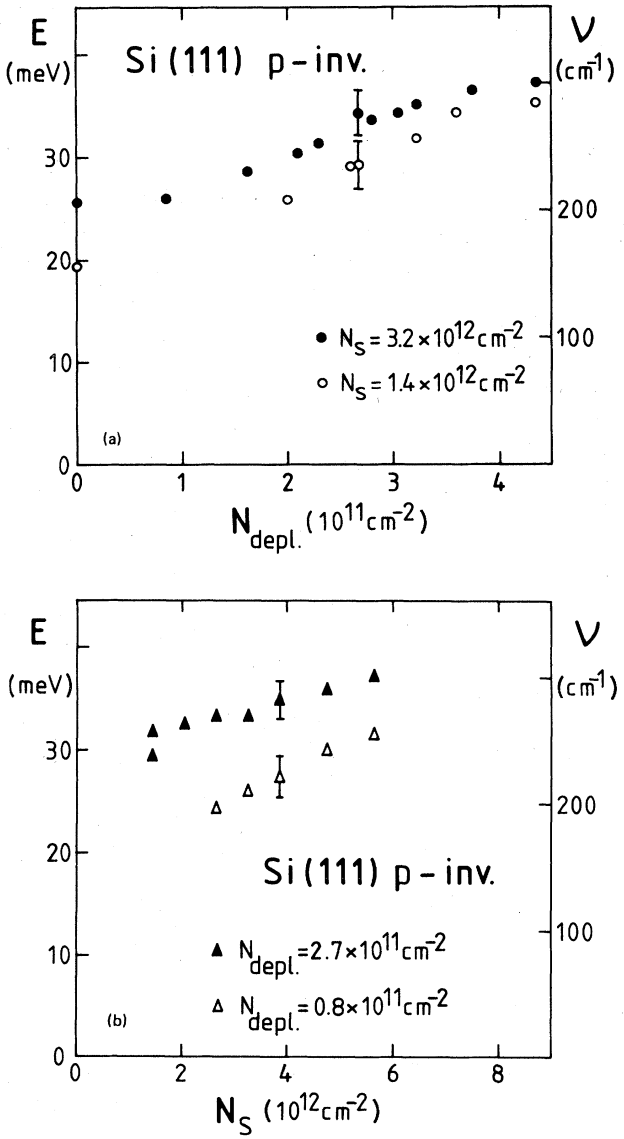

FIG. 3. Dependence of the intersubband-resonance positions for Si(111) on (a) the depletion charge N_{depl} for fixed N_s, and (b) on the charge density N_s for fixed N_{depl}.

lation conditions. This suggests nonparabolicity as the main broadening effect.

In Fig. 3 we show the influence of the depletion field on the position of the main resonance. As expected, we find the influence of the depletion charge to be smaller for larger inversion carrier densities N_s. Quantitative calculations for the influence of depletion fields on the hole subband structure are not available. Experimental data published for low densities on Si(100) show no difference between accumulation and inversion.[6] For low densities on Si(110), a difference in the resonance position has been found upon comparing accumulation and inversion.[11] The difference is comparable with an extrapolation of our results for Si(111) to lower densities.

We have also performed some experiments at different temperatures. At 80 K there is a shift of the resonance position of about 5 meV to higher energies. Although the resonance half-width is not significantly affected, the resonance amplitude decreases by about 20%. At room temperature, intersubband transitions give a weak and broad contribution which can hardly be separated from the Drude background.

3. Si(100)

Experimental spectra for the accumulation of holes on Si(100) are shown in Fig. 4. To increase the visibility of small features in the traces for the different N_s, particularly at the shoulder of the resonance, we have smoothed the original curves where necessary. The noise level is indicated in the caption. The spectra are similar to those of the Si(111) surface in Fig. 1 with relatively broad resonances. The low-energy resonance structure at the shoulder is more separated from the main resonance in Si(100) than in Si(111). At the same density, resonance positions for Si(100) are about 50 cm^{-1} higher in energy compared with Si(111), and the excitation strength is significantly lower by about a factor of 2.

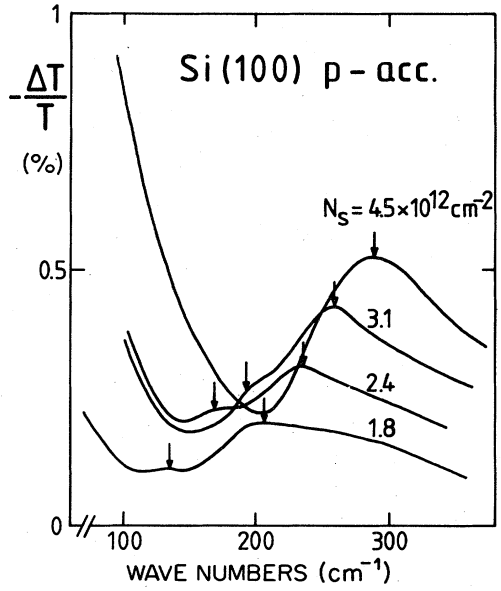

FIG. 4. Experimental spectra $-\Delta T/T$ versus wave number for accumulation layers of holes on Si(100). The intersubband-resonance positions for the different densities N_s are marked by arrows. Peak-to-peak noise level for $\Delta T/T$ is, e.g., for 200 cm^{-1} and $N_s = 3.1\times10^{-12}$ cm^{-2}, 0.04%.

4. Si(110)

Experimental spectra for a typical Si(110) sample are shown in Fig. 5. In contrast to Si(100) and Si(111), the spectra on this surface depend strongly on the polarization of the incident radiation. This anisotropy reflects the twofold rotational symmetry of the (110) surface. The difference in the Drude absorption for linear polarization in [$\bar{1}$10] and [001] directions is due mainly to the difference in the optical mass of both directions.[22] Figure 5 also indicates that, for both directions of polarization, the excitation strength of the intersubband resonance is different and also does not scale with the Drude background. The resonance position is nearly the same for both directions of polarization, but, for all samples measured, there is a tendency that the peak position for the [001] direction is shifted by about 10 cm^{-1} to higher wave numbers with respect to the peak position of the [$\bar{1}$10] direction. On the Si(110) surface it is also possible to detect very weakly excited intersubband resonances at low energies. In the direct spectra $\Delta T/T$ these resonances can hardly be separated from the frequency-dependent Drude background. If one divides the spectra for both directions of polarization, the Drude-type intraband transitions should essentially reflect the frequency-independent reciprocal mass ratio. However, due to the different excitation strength of the intersubband transitions, this second resonance is clearly resolved in the divided spectra[20] and the

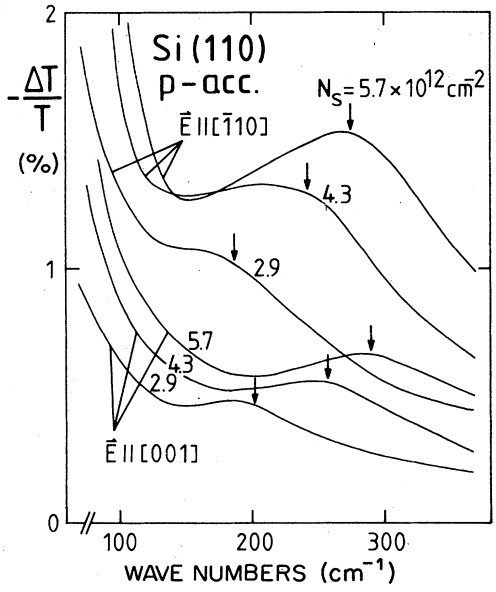

FIG. 5. Experimental spectra $-\Delta T/T$ versus wave number for accumulation layers of holes on Si(110). Spectra are measured with linearly polarized light. The direction of the electric field vector in the surface is indicated. Intersubband-resonance positions are marked by arrows. Typical peak-to-peak noise levels are 0.05%.

positions agree with laser-spectroscopic measurements on the same sample.

For inversion and substrate-bias conditions on Si(110) the asymmetry for different polarizations becomes more pronounced. Additionally, fine structures can be observed within the main resonance, which indicates that this resonance consists of different, partly overlapping transitions.

5. *Absolute excitation strength of hole intersubband resonances*

From our measurements we can extract the change in transmission $\Delta T/T$ in absolute units, and thus determine the real part of the high-frequency conductivity $\mathrm{Re}[\sigma(\omega)]$ by inserting the gate impedance and dielectric function of Si (see formulas in Refs. 19 and 20). In the low-signal approximation and for typical gate impedances of 500—1000 Ω, as in our experiments, $-\Delta T/T$ has to be divided by 150 to give the real part of $\sigma(\omega)$ in units of Ω^{-1}. To characterize the excitation strength of the intersubband resonance, here we will discuss the peak amplitude of the main resonance. The Drude background is subtracted. It is not possible to give the integrated intensity of the resonance profile, since, especially at high densities, the entire profile is not within the spectral range of the detector used in this experiment. On the other hand, the half-width is similar for all surfaces.

We find that for densities $N_s \gtrsim 2\times10^{12}$ cm^{-2} the peak amplitude increases roughly (within $\pm20\%$) in proportion with N_s, with a tendency to saturation at higher N_s. Within the same accuracy, measurements on different samples from different batches, substrate doping, and manufacturers give identical results. Typical mean values for the peak amplitude of $-\Delta T/T$ at a density of $N_s=5\times10^{12}$ cm^{-2} are 0.8% for Si(111), 0.35% for Si(100), and 0.35% and 0.65% for Si(110) and polarization parallel to [001] and [$\bar{1}$10], respectively.

These values are measured on samples with intraband scattering times τ of typically $(1-3)\times10^{-13}$ s. For these values of τ, the excitation strengths on different samples of a given surface orientation are identical within $\pm20\%$. Thus we cannot conclude from our experiments that an increase of τ yields a higher excitation strength. The low-energy structures on the shoulder of the main resonance observed on Si(111) and Si(100) surfaces are slightly differently pronounced in the spectra of different samples, but we cannot find any correlation of this with τ.

B. Resonance positions in comparison with theory and other experiments

Before we discuss the details of the hole intersubband dispersion, we briefly recall the present theoretical understanding of the 2D hole subband system of Si. Self-consistent Hartree calculations of hole subband energies have been performed independently by Bangert *et al.*[8] and by Ohkawa *et al.*[9] Many-body corrections, which are not included in Refs. 8 and 9, are treated in a rough approximation for low densities on Si(100).[10] The main features of these results are the following. The three valence bands of the bulk mix under the influence of the surface electric field and form a system of subbands. We follow the notation of Bangert *et al.*[8] and characterize the subbands as heavy (index h), light (l), and spin-orbit-split-off bands (s.o.). If no clear assignment is possible, the bands are labeled "not identified" (n.i.). On all three surfaces the lowest subband is a heavy-hole subband (h_0), followed by a light-hole subband (l_0), and another heavy-hole subband (h_1). It is characteristic for hole subband systems that, starting at relatively low charge densities [$N_s\approx(2-3)\times10^{12}$ cm^{-2}], the second subband l_0 will be occupied, even at $T=0$. Each band splits for $\vec{k}_{\|}\neq\vec{0}$. At a given $\vec{k}_{\|}\neq\vec{0}$, the wave functions of the two corresponding eigenstates are composed from different combinations of the spin orientation with respect to the orbital motion. We refer to these eigenstates as "quasispin states." The lifting of the quasispin degeneracy is an inherent feature of systems without inversion symmetry. It is caused by the influence of an asymmetric potential on the spin-orbit interaction. Such lifting has recently been observed in heterostructures.[23,24] The subbands are strongly nonparabolic with different dispersions and curvatures for different subband indices and quasispin states. The energy contours in the k_x-k_y plane are warped. Both calculations[8,9] use essentially the same formalism, but they differ slightly in the choice of the trial functions. They give similar results for the cyclotron mass;[25] however, subband energies and subband separations of both calculations differ significantly (see Figs. 6—8).

For a comparison of experimental intersubband energies with these calculations, one must bear in mind the following limitations. (1) Calculations[8,9] do not include many-body corrections, which, however, might not be important at high densities. (2) The image potential is not included, except for the case of the Si(111) surface discussed in Ref. 9. (3) Calculations are performed for inversion ($N_{\mathrm{depl}}=1.2\times10^{11}$ cm^{-2}). We will discuss accumulation data, but, as shown in Fig. 3, the difference between inversion and accumulation is small, with inversion data being less than 2 meV above accumulation data for $N_s>2\times10^{12}$ cm^{-2}. (4) A very important and probably very crucial point is that calculated subband separations are only available for $\vec{k}=\vec{0}$. For an exact comparison one must integrate subband transitions from all occupied $\vec{k}$ states. Furthermore, the density of states and the $\vec{k}$ dependence of the matrix elements must be taken into account to describe the resonance position and line shape correctly. (5) Intersubband-resonance positions differ from subband separations due to depolarization effects and final-state interactions (e.g., Refs. 1 and 2). Because of the symmetry of the hole energy contours, depolarization shifts are not expected for our data in parallel excitation. The interesting question of the effectiveness of depolarization effects for perpendicular excitation in the strongly nonparabolic hole subband system will not be treated in our paper. Final-state interactions should be present in our experimental data, but as yet, no theoretical treatment of final-state effects in nonparabolic subband systems with many closely separated bands exists.

We expect that the most pronounced resonances, starting at low densities, should correspond to transitions from the lowest subband, the h_0 band. Transitions from the l_0

band should not be present below a certain density N_{sl_0}, where the l_0 band is not occupied. On the other hand, $h_0 \rightarrow l_0$ transitions are also possible at densities above N_{sl_0}, since there are empty l_0 states at higher $\vec{k}$ vectors.

Our experimental hole intersubband-resonance positions for Si(111) are summarized in Fig. 6. Different symbols indicate measurements on samples from different wafers. We have measured intersubband resonances on both n- and p-type samples and for substrate doping ranging from 10^{13} to 5×10^{15} cm^{-3}, without any significant difference in resonance position. The main resonances are about 10 meV below the $h_0 \rightarrow h_1$ subband separation of Ref. 8, and the high-energy transition is about 10 meV above the $h_0 \rightarrow h_2$ separation. Good coincidence of the low-energy shoulder with the $l_0 \rightarrow h_1$ separation exists. Comparison with theoretical data of Ref. 9 shows rather good agreement of the main resonance with the $h_0 \rightarrow h_1$ separation, but the low-energy shoulder has to be compared with a $h_0 \rightarrow l_0$ separation.

For Si(100) in Fig. 7 both the main resonance and the low-energy shoulder are at low densities about 10 meV below the $h_0 \rightarrow h_1$ and the $l_0 \rightarrow h_1$ separations of Ref. 8, respectively. Better coincidence exists at low densities with the $h_0 \rightarrow h_1$ and $l_0 \rightarrow h_1$ separations of Ref. 9. For densities above 3×10^{12} cm^{-2}, however, the experimental main resonance shows a much slower increase than the theoretical N_s dependence.

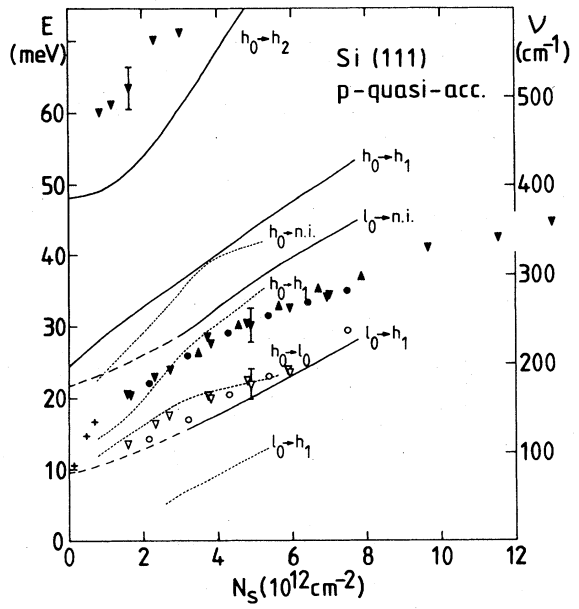

FIG. 6. Experimental hole intersubband-resonance positions for accumulation layers on Si(111). Different symbols indicate measurements on samples from different wafers (see text). Theoretical subband separations are indicated by solid (Ref. 8) and dotted lines (Ref. 9) and are labeled with the corresponding transition. Dashed parts of the lines (Ref. 8) indicate the charge-density regime where transitions from the l_0 subband are not possible since this band is not occupied at low densities. Pluses (+'s) mark experimental data points from Ref. 11.

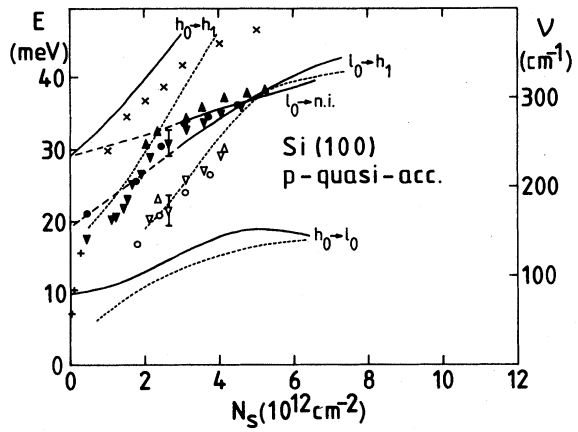

FIG. 7. Experimental hole intersubband-resonance positions for accumulation layers on Si(100). For further explanation, see Fig. 6. Pluses (+'s) mark experimental data points from Ref. 6 measured by far-infrared laser spectroscopy. Crosses (×'s) mark experimental resonance positions from Raman experiments (Ref. 12).

For Si(110) in Fig. 8 the main resonance position is about 15 meV below the $h_0 \rightarrow h_1$ separation of Ref. 8, but perhaps this resonance also includes $h_0 \rightarrow l_0$ and $l_0 \rightarrow$ s.o. transitions, which are very closely separated according to Ref. 8. This is also suggested from inversion experiments, where additional structures are found within the main resonance. Rather good coincidence exists for the main resonance and the $h_0 \rightarrow h_1$ separation of Ref. 9. The low-energy transition, however, agrees well with the $l_0 \rightarrow h_1$ separation of Ref. 8, whereas no identification with data from Ref. 9 is possible.

An important quantity in subband systems is the onset of the occupation of higher subbands with increasing charge density. For Si(110), Ohkawa *et al.*[9] calculated the

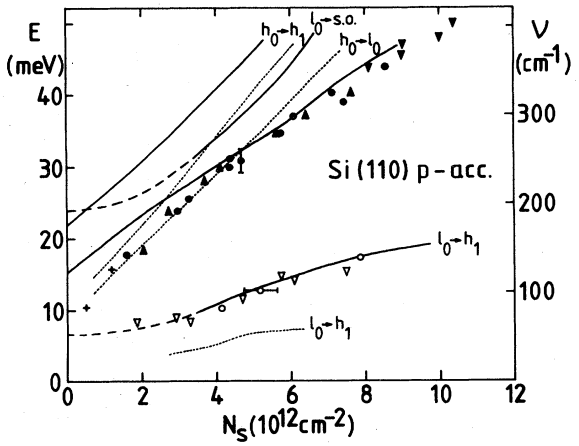

FIG. 8. Experimental hole intersubband-resonance positions for accumulation layers on Si(110). For further explanation, see Fig. 6. The low-energy resonances are extracted from laser spectroscopy (○) and from divided Fourier-transform spectra (△; see text). Pluses (+'s) mark experimental data from Ref. 11.

occupation of the l_0 subband to start at $N_s = 2.4 \times 10^{12}$ cm^{-2}, while Bangert *et al.*[8] found 3.7×10^{12} cm^{-2}. From Shubnikov–de Haas (SdH) experiments, values of 2.8×10^{12} (Ref. 26) and 2.2×10^{12} cm^{-12} (Ref. 27) have been deduced. From our samples, in SdH experiments we find a value of 2.6×10^{12} cm^{-2}. At this density, in an N_s sweep we also observe a structure in the Drude conductivity, indicating a change in mobility at the onset of the occupation of the l_0 subband.

We can draw the following conclusions from this comparison of theory and experiment. The theories[8,9] describe the qualitative features, e.g., nonparabolicity and closely separated bands, of the very complex hole subband system rather well. However, with the limitation of the currently available theoretical data in mind, which do not include many-body corrections, image potential, $\vec{k}$ dispersion, the $\vec{k}$ dependence of matrix elements, density of states, and final-state interactions, it is not possible to say how well the presently available theories describe the subband structure of holes quantitatively. It would be highly desirable if additional calculations were performed, particularly including the effects of $\vec{k}$ dispersion and the $\vec{k}$ dependence of the matrix elements, to explain the details of the great amount of experimental data now available, i.e., resonance positions, line shape, and excitation strength. This is not only applicable to intersubband transitions in Si, but is also of general interest. Depolarization effects in nonparabolic systems and final-state interactions in structures with closely separated bands are of further interest. Whether the lifting of the quasispin degeneracy is reflected in the experimental spectra and can thus be extracted from experiments is also worth studying. One might speculate whether the small and sharp low-energy resonance for Si(111) and Si(100) in Figs. 1 and 4 are perhaps caused by the lifting of the quasispin degeneracy. Available theoretical data[8] show that for one spin state the h_0 and h_1 subbands have relatively identical separations in $\vec{k}$ space, whereas for the other spin state both subbands have different dispersion curvatures, which would lead to a much broader resonance than for the first spin state.

We will now compare our resonance positions with experimental data from other workers. Far-infrared-absorption data are only available at low densities. For Si(100) we find that extrapolation of our main resonance positions to lower densities in Fig. 7 gives good agreement with experimental data from Ref. 6. For Si(111) (Fig. 6) and Si(110) (Fig. 8), good agreement with data from Ref. 11 can also be extrapolated. Comparison with experimental data from Raman spectroscopy[12–14] shows no general agreement. For certain surface orientations and density regimes there are significant differences in resonance positions. For Si(111), resonance positions in Ref. 14—which are measured up to 3×10^{12} cm^{-2}—agree with our main resonance. In addition, another transition is observed in a Raman experiment[14] about 12 meV above our main resonance, but no low-energy transitions corresponding to our $l_0 \rightarrow h_1$ data in Fig. 6 are observed in Ref. 14. For Si(100), Raman resonances[12,14] are about 10 to 15 meV above our main resonance positions (see Fig. 7). For Si(110), Raman resonance positions[14] start at 1×10^{12} cm^{-2} with the same energy as in our experiment (Fig. 8), but show a much steeper dispersion for increasing N_s than our experiments. Low-energy resonances[14] are about 10 meV above values in our spectra. Although the ratio of intersubband-resonance amplitude to background is in most cases much lower in Raman experiments, we do not think that differences in evaluating the resonance positions explain these significant differences. One reason might be that the $\vec{k}$ dependence of the excitation strength for Raman experiments, which include a spin-flip process, and for far-infrared excitation, is different, which implies that the resulting resonance positions of the transitions between nonparabolic bands of all $\vec{k}$ vectors are different. Furthermore, it is not clear whether the rather strong illumination of the sample in Raman spectroscopy might be the origin of a different behavior.

IV. PARALLEL EXCITATION OF INTERSUBBAND RESONANCES IN ELECTRON SPACE-CHARGE LAYERS

For electron subbands on Si, considerably more information exists than for holes. For the Si(100) surface, many-body corrections, depolarization, and final-state interactions are relatively well understood both theoretically and experimentally (e.g., Ref. 1). Owing to the symmetry, intersubband transitions cannot be excited in parallel excitation on Si(100), but for Si(110) and Si(111) the ellipsoidal energy contours of the bulk are tilted with respect to the surface and therefore the motion of subband electrons parallel and normal to the surface is coupled (e.g., Refs. 17 and 18). So far, subband spectroscopy on these

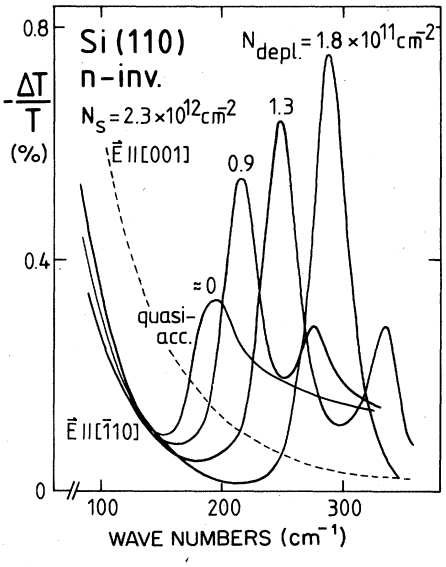

FIG. 9. Experimental spectra $-\Delta T/T$ versus wave number for accumulation, inversion, and different depletion fields (indicated by the depletion charge N_{depl}) of electrons on Si(110). For normally incident radiation, the intersubband resonance can only be excited with polarization of the electric field vector parallel [$\bar{1}10$]. For polarization parallel to the direction [001] (dashed line) the spectrum is Drude type without intersubband contributions. The typical peak-to-peak noise level is 0.03%.

surfaces has been limited to low densities and energies (e.g., Refs. 28–30), except for recent experiments that have been carried out parallel to ours.[31–33] The purpose of this section is to give a survey of our frequency-domain study of electron intersubband resonances in parallel excitation for a large frequency and charge-density regime, and with special emphasis on the differences in the behavior for accumulation, inversion, or substrate-bias conditions, respectively.

A. Si(110)

Experimental spectra for accumulation, inversion, and some substrate-bias voltages in electron space-charge layers on Si(110) are shown in Fig. 9. A significant feature is the strong anisotropy for different polarizations of the electric field vector in the surface. The anisotropy of the Drude background is proportional to the reciprocal optical mass of the corresponding directions, as has also been found in plasmon-resonance experiments.[34] Intersubband resonances are only observed for polarization of the electric field vector parallel to [$\bar{1}$10] since the energy ellipsoids are tilted in this direction. The intersubband resonance for accumulation conditions in Fig. 9 is rather broad and asymmetric. This is caused by transitions from the ground subband E_0 to a continuum of higher subbands E_i ($i>0$) and reflects the relative shallow accumulation potential. For inversion conditions the line shape changes drastically (in contrast to hole intersubband resonances; see Fig. 2). The line profile becomes symmetric and a second $E_0 \rightarrow E_2$ transition is well separated. The peak and integrated excitation strength is increased and the energetic half-width $\Delta E = 6$ meV corresponds, within about 20%, with the value of $2\hbar/\tau$, where τ is the intrasubband scattering time, determined from a Drude fit to the background of the spectra on the same sample and the same density. With increasing substrate-bias voltage and corresponding depletion field, the $E_0 \rightarrow E_1$ and the $E_0 \rightarrow E_2$ transitions shift to higher wave numbers, the resonance half-width decreases slightly, and the peak amplitude increases. We have checked carefully, using different methods (measuring the charging current, investigation of the Drude background, and changing the time between recharging the sample[20]), that the charge density N_s remains constant during the time that the substrate-bias voltage is applied. Thus, the resonance shift and amplitude enhancement in Fig. 9 is not caused by an increase of N_s. The increase of the resonance energy with increasing substrate-bias voltage is caused by the narrowing of the surface potential well with an additional depletion field, which leads to a larger subband separation. We interpret the increase of the excitation strengths for higher depletion fields by a stronger overlapping of the electron wave functions. In particular, the depletion field causes a narrowing of the extension for the wave functions of the higher subbands, while the ground subband is less affected. Thus the dipole matrix element, which governs the intersubband excitation strengths, increases for higher depletion fields.

It is interesting to compare our experimental line shapes with calculations by Ando *et al.*[17] since this sheds light on the problem of the valley degeneracy on Si(110). From the effective-mass approximation the valley degeneracy should be $g_v = 4$. However, in Shubnikov–de Haas experiments a value of $g_v = 2$ has been found. There has been extensive discussion in the literature (see e.g., Refs. 1 and 35) as to whether the lifting of the valley degeneracy is real or only simulated in the SdH measurements. According to Ref. 17 depolarization effects become effective for $g_v = 2$; excitonlike effects also depend on the value of g_v. Our experimental line shape of the electron intersubband resonance on Si(110) for accumulation agrees much better with the theoretical line shape[17] for $g_v = 4$ than that for $g_v = 2$. The calculated[17] ratio of the intersubband amplitude for inversion compared to that for accumulation is 1.5 for $g_v = 4$ and 2.2 for $g_v = 2$. If we extrapolate our experimental results to the conditions of these calculations, we find a value of 1.6, which also seems to favor a degeneracy of $g_v = 4$. On the other hand, SdH measurements on the same samples seem to indicate a degeneracy of 2. From our experiments we see evidence that the real valley degeneracy is $g_v = 4$ and the value of 2 in SdH measurements is simulated, as proposed in the model of Ref. 35. $g_v = 4$ also implies that our resonance positions are not depolarization-shifted. $g_v = 4$ has also been deduced from a comparison of parallel and perpendicular excited intersubband resonances,[32,33] and has been very recently demonstrated for SdH measurements as well.[36]

Figure 10 shows experimental intersubband resonances for electron inversion on Si(110) at different charge densities N_s. Both the $E_0 \rightarrow E_1$ and the $E_0 \rightarrow E_2$ resonances shift with increasing N_s to higher wave numbers, the resonance amplitude increases with N_s, and the resonance half-width remains nearly unaffected in this density re-

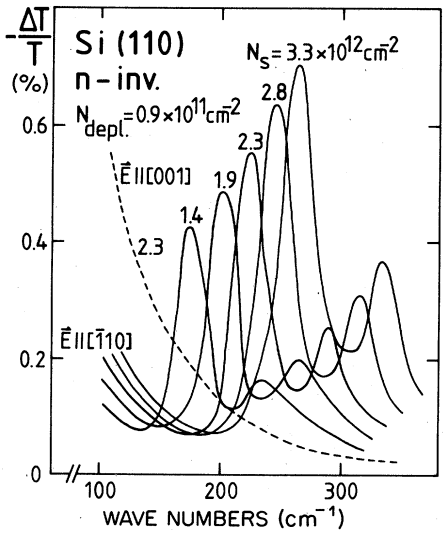

FIG. 10. Experimental spectra $-\Delta T/T$ for electron inversion on Si(110) at different charge densities N_s. The radiation is linearly polarized parallel to the [$\bar{1}$10] direction, except for the dashed line, which shows the spectra for $N_s = 2.3 \times 10^{12}$ cm^{-2} and polarization parallel to the [001] direction. The peak-to-peak noise level is typically 0.05%.

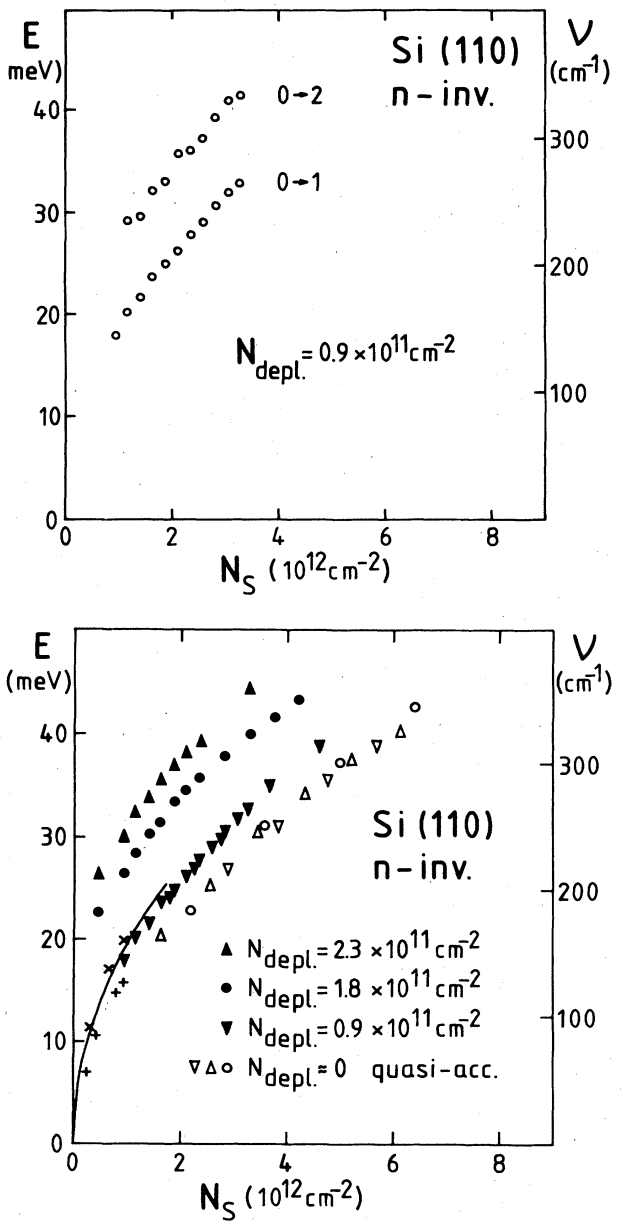

FIG. 11. Experimental electron intersubband-resonance positions on Si(110). (a) Dispersion of the $E_0 \rightarrow E_1$ and the $E_0 \rightarrow E_2$ transition for inversion. (b) Dispersion of the $E_0 \rightarrow E_1$ transition for accumulation and different depletion fields indicated by the depletion charge N_{depl}. The experimental accuracy is of the size of the symbols. Solid line shows calculated resonance positions (Ref. 37) for $N_{\text{depl}} = 6 \times 10^9$ cm^{-2}. Pluses and crosses (+ 's and ×'s) mark experimental data from Refs. 39 and 29, respectively.

gime. In contrast to Fig. 9, the increase of intensity is caused, in this case, by the increasing number of charge carriers N_s. Experimental resonance positions for electron intersubband resonance on Si(110) are summarized in Fig. 11. The dependence of the $E_0 \rightarrow E_1$ and the $E_0 \rightarrow E_2$ transitions on the charge density N_s is plotted in Fig. 11(a). Both resonance energies increase with N_s, and the $E_0 \rightarrow E_2$ transition is constantly about 9 meV above the $E_0 \rightarrow E_1$ energy. This experimental value of 9 meV is significantly lower than the calculated value of 15 meV in the model of Ref. 17, where nearly the same depletion charge has been used. The experimental $E_0 \rightarrow E_1$ transition energies for different depletion fields are summarized in Fig. 11(b). Accumulation data are clearly lower in energy than inversion data ($N_{\text{depl}} = 0.9 \times 10^{11}$ cm^{-2}). Inversion data agree with calculated resonance positions at low densities in Ref. 37. For very recent calculations,[38] surprisingly, the Hartree approximation gives the best agreement with our experimental results. The theoretical data are about 2 meV above our experiment resonance energies for $N_{\text{depl}} = 1 \times 10^{11}$ cm^{-2}. However, the theoretical data for local-density-functional and many-body perturbational calculations are significantly (10—15 meV) higher in energy than our data. Extrapolation of our results to lower densities agrees with experimental data for inversion[29] and accumulation.[39] Good agreement is also found with recent accumulation data for a larger charge-density regime.[31]

B. Si(111)

Experimental spectra for accumulation layers of electrons on Si(111) are shown in Fig. 12. The intersubband-resonance profile is broad and asymmetric, as is typical for accumulation in electron space-charge layers [see discussion above for Si(110)]. The absolute excitation strength is weaker than for accumulation of electrons on Si(110). The spectra are within the experimental accuracy identical for polarization parallel to the [$\bar{1}\bar{1}2$] and [$\bar{1}10$] directions. This is consistent with a sixfold valley degeneracy. We performed some exemplary measurements for inversion of electrons on Si(111). The spectra are similar to those of the Si(110) surface in Fig. 9, e.g., for

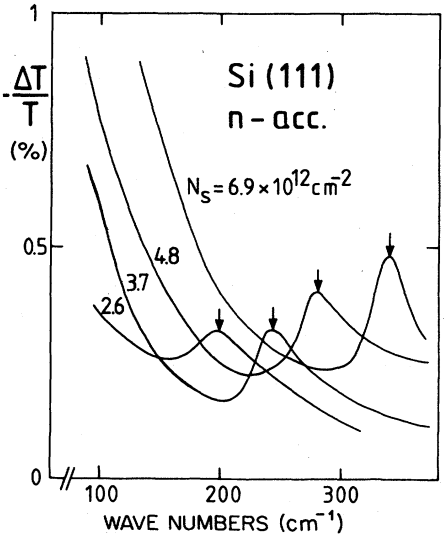

FIG. 12. Experimental spectra $-\Delta T/T$ versus wave number for accumulation layers of electrons on Si(111). The typical peak-to-peak noise level is 0.06%.

$N_s = 3.0 \times 10^{12}$ cm^{-2} and $N_{\text{depl}} = 1.7 \times 10^{11}$ cm^{-2} the $E_0 \rightarrow E_1$ transition is at 32 meV, 5 meV above the accumulation resonance, the $E_0 \rightarrow E_2$ resonance energy is at 43 meV, and the $E_0 \rightarrow E_1$ half-width is 5 meV.

Resonance positions for different typical samples are summarized in Fig. 13. Extrapolation of our data to low densities agrees with experimental data in Ref. 39 and with resonance positions in Ref. 30, which have been characterized as "accumulationlike" ($g_v = 6$). Good agreement is also found with recent accumulation measurements for a larger charge-density regime.[32] Calculated values[37] for low depletion charges ($N_{\text{depl}} = 6 \times 10^9$ cm^{-2}) are slightly higher than our accumulation data, as shown in Fig. 13. Recent calculations in Ref. 18, however, give much higher resonance energies, and comparison with theoretical data in Ref. 38 leads to the same discrepancies that have been discussed above concerning this reference for Si(110).

C. Additional remarks

We note here that our electron intersubband-resonance experiments on both Si(110) and Si(111) were performed on samples which were prepared using standard processes (see acknowledgments). Samples from different batches and manufacturers show identical results. Only on some Si(111) samples, which exhibit a mobility below 300 cm^2 V^{-1} s^{-1}, are the excitation strengths low and the resonance positions about 5 meV below the accumulation data of "normal" samples. (It is possible that the lowering of the resonance energy on low-mobility samples is caused by impurity scattering, which will lead, according to Ref. 38, to a reduction of the exchange-correlation corrections and thus of the subband energy separation.) SdH measurements on the "normal" samples of both Si(110) and Si(111) seem to indicate a degeneracy of 2. However, as discussed above, line-shape analysis suggests that $g_v = 4$ for our Si(110) samples. Furthermore, for Si(111), plasmon experiments on the same samples give strong evidence that $g_v = 6$.[40] Thus we think that $g_v = 2$ is simulated in SdH experiments. Further information on the valley degeneracy could be achieved by comparing data for parallel and perpendicular excitation. Here we will refer the reader to other papers.[18,32,33]

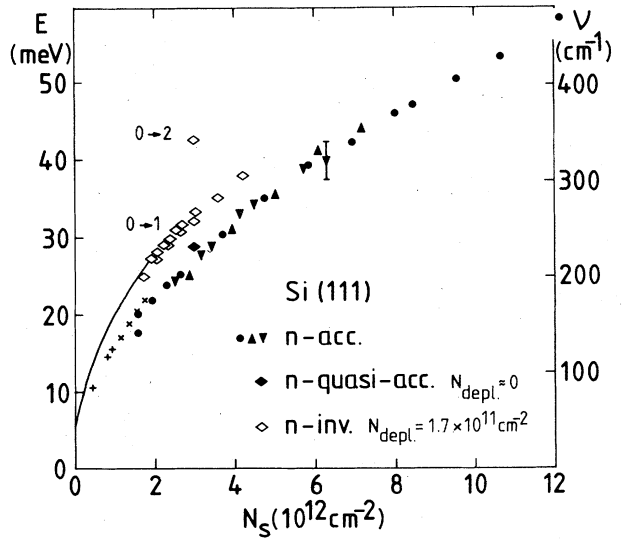

FIG. 13. Experimental intersubband-resonance positions for space-charge layers of electrons on Si(111). Solid lines indicate theoretical resonance energies (Ref. 37) for $N_{\text{depl}} = 6 \times 10^9$ cm^{-2}. Pluses and crosses (+ 's and ×'s) mark experimental data from Refs. 39 and 30, respectively.

We would like to draw attention to the following surprising fact. Although there are significant differences in the excitation strengths and polarization dependence, both Si(110) and Si(111) have, at the same density and within 1 meV, identical intersubband-resonance energies for accumulation of electrons. This statement is valid for the entire charge-density regime covered in Figs. 11(b) and 13. Surprisingly, our experimental resonance positions for parallel excitation on Si(110) also coincide within 10% with theoretical data[37] on Si(100) available for $N_s = (1-3) \times 10^{12}$ cm^{-2}. (Our comparison is with data calculated without a depolarization shift and for the same N_{depl} as in experiment.) Thus, the experimental electron intersubband energy dependence on N_s is nearly identical on all three principal surfaces of Si for the charge-density regime discussed here. In the very simple model of a triangular well (e.g., Ref. 1), the subband energies should be proportional to $m_z^{-1/3}$, where m_z is the perpendicular effective mass of the surface. In this model the resonance energy for the (110) surface should be 93% and, for the (100) surface, 65% of the resonance energy for Si(111), at the same density. Our experimental resonance positions on Si(111) and Si(110) coincide at the same density within experimental accuracy ($< 5\%$). Even more pronounced is the failure of this model to explain the coincidence of the data for Si(100) with the data for Si(110) and Si(111). This indicates that in the density regime treated here, this model is not even good enough to explain trends in subband energies if one compares different surfaces. Near coincidence of the intersubband dispersion for electron accumulation on the three principal surfaces of Si can also be found by comparing the theoretical data in Ref. 37. This coincidence has not been mentioned or discussed explicitly in Ref. 37. In Ref. 38 it has been stated that self-energy corrections are substantially insensitive to the surface orientation for Si(110) and Si(111), and also to the valley degeneracy $g_v = 2$, 4, or 6. However, as long as the calculations of intersubband-resonance energies with different methods lead to very different results (compare Refs. 37, 17, 18, and 38), one can not conclusively decide whether the coincidence of intersubband dispersions is an accident or the consequence of a more general principle.

Finally, we note that additional structures in the resonance profile of hole and electron intersubband transitions are observed in our measurements at high wave numbers (see resonance positions in Fig. 6 above 60 meV). Fano-type resonances and antiresonances occur and indicate interaction with phonons. These phenomena are currently under investigation and will be published separately.

V. CONCLUSIONS

We have presented frequency-domain studies of intersubband resonances in parallel excitation for electrons on Si(110) and Si(111) and for holes on Si(111), Si(100), and Si(110). We have investigated resonance positions, resonance line shapes, absolute excitation strengths, polarization dependence, and the influence of depletion fields in substrate-bias experiments.

Resonance positions for electron subbands agree, as far as available, with experimental results from other workers. Some of the published calculations explain our experimental resonance positions for electron subbands quite well, whereas others show significant differences. Thus a conclusive theoretical understanding does not exist. A line-shape analysis of the electron intersubband resonance on Si(110) suggests a valley degeneracy of 4 for this surface.

For hole intersubband-resonance positions, good agreement is found with available data from far-infrared measurements at low densities, but significant differences exist in comparison with data from Raman experiments. Our measurements of the hole intersubband resonance reflect the main features of the currently available theories, e.g., the existence of a number of different bands and the strong nonparabolicity. However, a quantitative comparison is not possible at the moment since important contributions are not included in the published theories, e.g., many-body interaction, image potential, integration of $\vec{k}$ dispersion and matrix elements in $\vec{k}$ space, depolarization shifts, and final-state interactions. These questions are of general interest for nonparabolic, multiband, and spin-degeneracy-lifted systems, and we hope that our experimental data will stimulate further theoretical treatments.

ACKNOWLEDGMENTS

We thank F. Koch for valuable discussions, W. Beinvogl of Siemens, Munich, and R. Wagner of the U. S. Naval Research Laboratory (Washington, D.C.) for supplying Si wafers. We thank the Deutsche Forschungsgemeinschaft for financial support.

[1]For a recent review, see T. Ando, A. B. Fowler, and F. Stern, Rev. Mod. Phys. **54**, 437 (1982).
[2]J. F. Koch, Surf. Sci. **58**, 104 (1976).
[3]F. Stern, Crit. Rev. Solid State Sci. **4**, 499 (1974).
[4]T. Ando, Phys. Rev. B **13**, 3468 (1976).
[5]B. Vinter, Phys. Rev. B **13**, 4447 (1976).
[6]P. Kneschaurek, A. Kamgar, and J. F. Koch, Phys. Rev. B **14**, 1610 (1976).
[7]B. D. McCombe, R. T. Holm, and D. E. Schafer, Solid State Commun. **32**, 603 (1979).
[8]E. Bangert, K. v. Klitzing, and G. Landwehr, in *Proceedings of the 12th International Conference on the Physics of Semiconductors, Stuttgart,* edited by M. H. Pilkuhn (Teubner, Stuttgart, 1974), p. 714; E. Bangert (unpublished).
[9]F. J. Ohkawa and Y. Uemura, Prog. Theor. Phys. Suppl. **57**, 164 (1975).
[10]F. J. Ohkawa, J. Phys. Soc. Jpn. **41**, 122 (1976).
[11]A. Kamgar, Solid State Commun. **21**, 823 (1977).
[12]G. Abstreiter, U. Claessen, and G. Tränkle, Solid State Commun. **44**, 673 (1982).
[13]M. Baumgartner and G. Abstreiter, Surf. Sci. (to be published).
[14]M. Baumgartner, G. Abstreiter, and E. Bangert, J. Phys. C **17**, 1617 (1984).
[15]A. D. Wieck, E. Batke, D. Heitmann, and J. P. Kotthaus, Surf. Sci. (to be published).
[16]D. Heitmann, J. P. Kotthaus, and E. G. Mohr, Solid State Commun. **44**, 715 (1982).
[17]T. Ando, T. Eda, and M. Nakayama, Solid State Commun. **23**, 751 (1977).
[18]K. S. Yi and J. J. Quinn, Phys. Rev. B **27**, 2396 (1983).
[19]D. C. Tsui, S. J. Allen, Jr., R. A. Logan, A. Kamgar, and S. N. Coppersmith, Surf. Sci. **73**, 419 (1978).
[20]E. Batke and D. Heitmann, Infrared Phys. (to be published).
[21]We calculated N_{depl} from the known formula (e.g., p. 619, Ref. 1). We estimated the accuracy of determining N_{depl} in this way to be better than 20%.
[22]E. Batke, D. Heitmann, A. D. Wieck, and J. P. Kotthaus, Solid State Commun. **46**, 269 (1983).
[23]H. L. Störmer, Z. Schlesinger, A. Chang, D. C. Tsui, A. C. Gossard, and W. Wiegmann, Phys. Rev. Lett. **51**, 126 (1983).
[24]D. Stein, K. v. Klitzing, and G. Weimann, Phys. Rev. Lett. **51**, 130 (1983).
[25]J. P. Kotthaus and R. Ranvaud, Phys. Rev. B **15**, 5758 (1977).
[26]K. v. Klitzing, G. Landwehr, and G. Dorda, Solid State Commun. **14**, 387 (1974).
[27]A. A. Lakhani, T. Cole, and P. J. Stiles, Solid State Commun. **39**, 569 (1981).
[28]T. Cole and B. D. McCombe, J. Phys. Soc. Jpn. Suppl. A **49**, 959 (1980).
[29]B. D. McCombe and T. Cole, Surf. Sci. **98**, 469 (1980).
[30]T. Cole, Surf. Sci. **113**, 41 (1982).
[31]Soe-Mie Nee, U. Claessen, and F. Koch, Phys. Rev. B **29**, 3449 (1984).
[32]F. Martelli, C. Mazuré, and F. Koch, Solid State Commun. **49**, 505 (1984).
[33]T. Cole and B. D. McCombe, Phys. Rev. B **29**, 3180 (1984).
[34]E. Batke and D. Heitmann, Solid State Commun. **47**, 819 (1983).
[35]B. Vinter and A. W. Overhauser, Phys. Rev. Lett. **44**, 47 (1980).
[36]K. C. Woo and P. J. Stiles, Phys. Rev. B **28**, 7101 (1983).
[37]T. Ando, Z. Phys. B **26**, 263 (1977).
[38]S. Das Sarma and B. Vinter, Phys. Rev. B **28**, 3629 (1983).
[39]A. Kamgar (unpublished).
[40]E. Batke, D. Heitmann, and J. P. Kotthaus, Surf. Sci. **113**, 367 (1982).